Effect of Poly(ADP-ribosyl)ation and Mg^{2+} Ions on Chromatin Structure Revealed by Scanning Force Microscopy†

Maria d'Erme,*,‡ Guoliang Yang,§ Eric Sheagly,|| Franco Palitti,‡ and Carlos Bustamante⊥

Department of Biochemical Sciences, University of "La Sapienza", P.le A. Moro 5, I-00185 Roma, Italy, Department of Physics, Drexel University, Philadelphia, Pennsylvania 19104, Institute of Molecular Biology, University of Oregon, Eugene, Oregon 97403, Department of Molecular and Cell Biology and Department of Physics, University of California, Berkeley, California 97420, and Physical Biosciences Division, Lawrence Berkeley National Laboratory, Berkeley, California 94720

Received December 1, 2000; Revised Manuscript Received May 8, 2001

ABSTRACT: Poly(ADP-ribosyl)ation of nuclear proteins is responsible for major changes in the high-order chromatin structure. The effects of this post-translation modification on nuclear architecture were examined at different Mg^{2+} concentrations using scanning force microscopy. A quantitative analysis of the internucleosomal distance, the width, and the volume of chromatin fibers imaged in tapping mode reveals that poly(ADP-ribosyl)ation induces a complete relaxation and decondensation of the chromatin structure. Our data, on the center-to-center distance between adjacent nucleosomes and on the fiber width, indicate that the poly(ADP-ribosyl)ated fibers remain significantly decondensed even in the presence of Mg^{2+}. Our results also show that the Mg^{2+} assumes an important role in the folding of chromatin structure, but Mg^{2+} is not able to restore the native feature of chromatin, when the fibers are depleted of H1/H5 histones. The combined effect of post-translation modification and cation ions on the chromatin structure shows that poly(ADP-ribosyl)ation could promote accessibility to DNA even in those nuclear processes that require Mg^{2+}.

The structure of the basic repeating unit of chromatin, the nucleosome, has been the subject of intense research during the past three decades.

In eukaryotic cells, the DNA is wrapped around the nucleosomes which are folded into high-order structure. Comparatively much less is known about the next level of organization of the chromatin fiber. Several models have been discussed concerning the arrangement of nucleosomes along condensed chromatin fibers. Significant studies, which included synchrotron X-ray scattering, cryoelectron microscopy (cryo-EM), and scanning force microscopy (SFM), have revealed that, at low and moderate ionic strengths, the fiber does not possess a regular structure as proposed in early models (*1*). In particular, under cryo-EM and SFM, the fibers seem to adopt irregular, extended structures 30−40 nm in diameter, in which the nucleosomes are arranged in a seemingly random three-dimensional "zigzag" fashion (*2*−*7*). These fibers are capable of adopting more condensed structures as the ionic strength is increased. It has been suggested (*5*, *6*) that these extended and more condensed irregular fiber structures may represent the extremes of the transcriptionally active and inactive forms of chromatin, respectively. In particular, compaction is induced through a reduction in the linker DNA entry−exit angle, leading to strengthening of the shaft structure (*8*). The form attained by chromatin during different states of the cell cycle appears to be influenced by post-translational modifications of nuclear proteins.

Despite the growing body of evidence accumulated in recent years about the role of the post-translational modifications, the manner in which these modifications induce condensation or decondensation of the chromatin fibers as a mechanism of controlling gene activities still remains an open question.

Poly(ADP-ribosyl)ation is a post-translational modification that occurs in the nuclei of eukaryotic cells. This modification is believed to result in a significant alteration of the chromatin structure through the addition of negative charges to various histone proteins (*9*, *10*). Poly(ADP-ribosyl)ation appears to be involved in several cellular events such as DNA repair, cell differentiation, apoptosis, tumor promotion, and histone function (*11*−*17*).

Poly(ADP-ribose) polymerase (PARP, EC 2.4.2.30), a zinc-binding nuclear enzyme, catalyzes the covalent addition and subsequent elongation of the ADP-ribose moiety of nicotinamide adenine dinucleotide (NAD) to proteins, to generate ADP-ribose polymers (*18*). Poly(ADP-ribose) is rapidly synthesized in the presence of DNA strand breaks, and it is then rapidly degraded by poly(ADP-ribose) glycohydrolase. The major acceptor proteins for poly(ADP-ribose) are the linker histone H1, core histones, and the enzyme molecule itself (*19*). In addition, it has been found that proteins involved in the breaking and rejoining of DNA strands, such as topoisomerases I and II, and ligase, as well

† M.d. has been supported by a CNR short-term mobility fellowship.

* To whom correspondence should be addressed: Department of Biochemical Sciences, University "La Sapienza", P.le A. Moro 5, I-00185 Roma, Italy. Fax: 39-06-4440062. E-mail: maria.derme@uniroma1.it.

‡ University of "La Sapienza".

§ Drexel University.

|| University of Oregon.

⊥ University of California and Lawrence Berkeley National Laboratory.

10.1021/bi002742a CCC: $20.00
Published on Web 08/21/2001

as HMG proteins involved in gene expression and nuclear matrix proteins, are also subjected to ADP-ribosylation (*20*−*23*).

Although the physiological role of poly(ADP-ribose)-polymerase is still unclear, this enzyme has been shown to play an important role in maintaining the genomic integrity, especially in those processes involving the base excision pathway of DNA repair (*12*). In addition, it is known that several proteins involved in DNA excision repair in higher eukaryotes undergo poly(ADP-ribosyl)ation. The most widely accepted view is that covalent linkage of ADP-ribose polymers is essential for the modification of the target protein function. The extent by which the protein function is modulated could, furthermore, depend on the number and size of ADP-ribose polymers incorporated (*24*). In vitro, histones can also bind ADP-ribose polymers noncovalently (*25*). Thus, it is conceivable that both types of linkages may contribute to alteration of DNA−histone interactions, thereby making the DNA accessible to DNA-processing enzymes, whereas the rapid degradation of the polymers by poly(ADP-ribose) glycohydrolase would allow histones and DNA to re-assemble (*26*). These dynamic processes could play a role in the modulation of histone type-specific polymer patterns and therefore modify chromatin functions (*27*).

Histone H1 is a key chromosomal protein involved in the stabilization of the nucleosome, and it is partly responsible for the organization of chromatin into higher-order structures (*28*). Poly(ADP-ribosyl)ation of histone H1 occurs via γ-carboxyl groups of glutamic acid residues in positions 2, 14, and 116 and the α-carboxyl group of the C-terminal lysine residue at position 213. These modifications could alter the electrostatic interactions between the positively charged N-terminal tails of H1 and DNA, thus changing the stability of the DNA−octamer association in the nucleosome (*29*), as well the cooperative interactions between H1 molecules (*30*). These events, and the interactions of the polyanionic groups of poly(ADP-ribose) with the positively charged tails of core histones, could lead to chromatin unfolding (*31*, *32*).

It has also been reported that the poly(ADP-ribosyl)ation process could be modulated by divalent cation concentration, which can itself affect the high-order chromatin structure (*33*−*36*). Thus, a complex interplay among all these factors may be involved in the modification of the chromatin fiber structure.

In the study reported here, the effects of poly(ADP-ribosyl)ation on chromatin condensation under different Mg^{2+} concentrations were investigated using scanning force microscopy (SFM). The center-to-center nucleosomal distance between adjacent nucleosomes was measured along with the width and the volume of chromatin fibers imaged in tapping mode SFM. These parameters were, then, used to characterize the structure of chromatin fibers prepared under different conditions.

EXPERIMENTAL PROCEDURES

Nuclei Isolation. Nuclei were isolated from chicken erythrocytes according to the procedure of Bordas (*2*). Briefly, chicken blood, from freshly slaughtered animals, was collected into 10% trisodium citrate to avoid clotting. After being filtered through eight layers of cheesecloth, the blood was centrifuged at 2500*g* for 10 min and resuspended in 2 volumes of buffer I [10 mM Tris-HCl (pH 7.5), 5 mM $MgCl_2$, and 10 mM NaCl]. After centrifugation, the pellets were lysed by gently stirring with 3 volumes of buffer I containing 0.5% NP 40. The lysates were centrifuged at 2500*g* and washed several times with buffer I. Nuclei were recovered and stored in buffer I containing 25% glycerol, at −20 °C. The temperature was kept constant at 4 °C throughout the preparation, and the extent of proteolysis was minimized by the presence of 1 mM phenylmethanesulfonyl fluoride (PMSF) (Sigma).

Isolation of Chromatin Fibers. Chromatin fibers were prepared according to the protocol of Libertini (*37*) with slight modifications. Nuclei were resuspended in buffer II (10 mM Tris-HCl, 150 mM NaCl, and 1 mM PMSF) to a DNA concentration of 60 A_{260} units/mL. Nuclei were digested with 10 units of micrococcus nuclease/mg of DNA in buffer II containing 1 mM $CaCl_2$ at 37 °C for 2−3 min. The digestion was terminated with the addition of 2 mM EDTA, and the digest was cooled on ice and centrifuged at 1500*g* for 5 min. The nuclei were lysed by slowly pipetting with 5 mM Tris-HCl (pH 7.5) and 1 mM EDTA, and the solubilized chromatin was collected by centrifugation at 8000*g* for 15 min.

Isolation of Stripped Chromatin Fibers. H1-depleted chromatin fibers were obtained by the method of Leuba (*5*). Soluble chromatin (4 mg/mL) was brought to 0.35 M NaCl, 10 mM Tris-HCl (pH 7.8), and 0.1 mM EDTA and added to 300 mg of CM Sephadex C-25. The mixture was shaken for 1 h at 4 °C. The chromatin−resin slurry was then loaded onto a CM Sephadex C-25 column (2.5 cm × 10 cm) prepackaged with 5 g of the same resin equilibrated with the same buffer. The stripped chromatin was eluted with the same buffer following the absorbance at 260 nm. The collected fractions were dialyzed against 10 mM Tris-HCl (pH 7.8) and 1 mM EDTA. The stripped chromatin fibers were incubated for 30 min in 10 mM Tris-HCl (pH 7.8) in the presence of 10 mM $MgCl_2$.

Purification and Assay of Poly(ADP-ribose) Polymerase. The enzyme was purified from chicken testis according to the procedure of Burtscher (*38*). Samples were incubated for 10 min at 30 °C in an assay buffer containing 100 mM Tris-HCl (pH 7.8), 10 mM $MgCl_2$, 0.5 mM dithiothreitol, 200 μM NAD, 2 μCi of [^{32}P]NAD (specific activity of 800 Ci/mmol) (NEN Life Science products), 2 μg of activated DNA, and 2 μg of histone H1. Enzymatic activity was determined from the amount of radioactivity incorporated from [^{32}P]NAD after precipitation with trichloroacetic acid (TCA) (*39*). An enzymatic unit is defined as 1500 pmol of ADP-ribose incorporated as tested in the standard assay.

Poly(ADP-ribosyl)ation of Chicken Erythrocyte Chromatin Fibers. Poly(ADP-ribosyl)ation of chromatin fibers (250 μg/mL, or 500 μg/mL determined from the A_{260} of DNA) was carried out for 15 min at 30 °C in a buffer containing 10 mM Tris-HCl (pH 7.8), 5 mM dithiothreitol, and 0.2 mM NAD, in the presence or absence of 5 units of poly(ADP-ribose) polymerase.

The reaction was stopped by the addition of 10 mM EDTA or 20 mM niacine. Chromatin fibers, under the same conditions, were also incubated with different $MgCl_2$ concentrations ranging from 2 to 10 mM. In parallel, chromatin fibers were poly(ADP-ribosyl)ated as described above, but

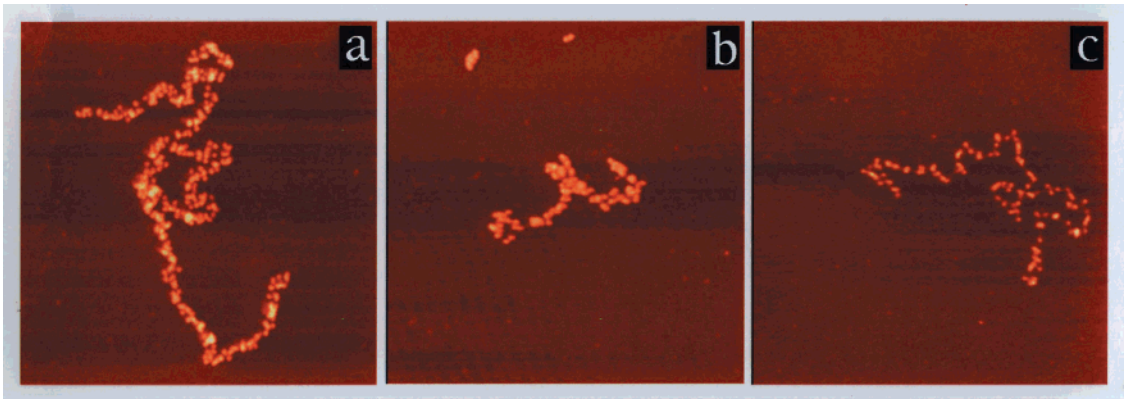

FIGURE 1: AFM images of chicken erythrocyte chromatin fibers. (a) Native chromatin fibers. (b) Endogenous poly(ADP-ribosyl)ated chromatin fibers. (c) Exogenous poly(ADP-ribosyl)ated chromatin fibers. All the samples are glutaraldehyde-fixed, deposited from 5 mM triethanolamine-HCl (pH 7.5) with 1 mM EDTA on mica, and imaged in air. Images were 1 μm × 1 μm in size. Heights are indicated by varying shades of color with low regions in dark reddish brown and higher regions in increasingly lighter tones toward yellow and white, over a range of 0−15 nm. The same color code was used for all images.

in the presence of 2 μCi of [^{32}P]NAD, precipitated with 25% TCA on ice, filtered with the HA filter, and used as controls.

Analysis of the DNA and Histone Content of the Chromatin Fibers. The DNA length of chromatin fibers was determined with a 1% agarose gel, and the protein content of the chromatin fibers and of the respective ADP-ribosylated samples was analyzed by 17% SDS−polyacrylamide gel electrophoresis, after precipitation with 25% TCA. Gels were stained with 0.1% Coommassie blue R-250, dried, and autoradiographed using Kodak X-ray film.

Isolation of ADP-Ribose Polymers from Chicken Erythrocyte Nuclei. Poly(ADP-ribose) was purified by the method of Malanga (*40*), and the polymer size distribution was analyzed by 20% polyacrylamide gel electrophoresis in 0.09 M Tris borate buffer (pH 8.3), according to the method of Panzeter and Althaus (*41*). The polymer size was expressed relative to the mobility of the dyes bromophenol blue (BBF) and xylene cyanol (XC) (*42*). The polymers resuspended in 10 mM Tris-HCl (pH 7.8), 5 mM dithiothreitol, and 1 mM EDTA were added to the soluble and depleted chromatin in ratios of 0.2:1, 0.5:1, and 1:1 (w:w), respectively.

Purification of H1/H5 Histones and Their Respective Poly-(ADP-ribosyl)ated Isoforms. Nuclei were incubated for 15 min at 30 °C in 10 mM Tris-HCl (pH 7.8) containing 5 mM dithiothreitol and 10 mM $MgCl_2$, in the presence or absence of 0.2 mM NAD and 74 μCi of [^{32}P]NAD. The reaction was stopped by the addition of 0.4 N H_2SO_4. H1/H5 histones and poly(ADP-ribosyl)ated isoforms were purified from chicken erythrocyte nuclei following the procedure of d'Erme (*43*).

Reconstitution of Depleted Chromatin with H1/H5 Histones and Its Respective Poly(ADP-ribosyl)ated Analogues. H1-depleted chromatin fibers were reconstituted by addition of H1/H5 histones or their respective poly(ADP-ribosyl)-ated analogues at ratios of 1:0.2, 1:0.5, 1:1, and 1:2 in a buffer containing 10 mM Tris-HCl (pH 7.8) and 1 mM EDTA as described by De Lucia (*44*).

Scanning Force Microscopy Analysis. Chromatin fiber samples prepared under different experimental conditions were dialyzed against 5 mM triethanolamine-HCl (TEA) at pH 7.5 and fixed overnight in 0.1% glutaraldehyde (*45*). The fibers were deposited on a fresh mica surface, gently washed with Nanopure water, and dried with nitrogen gas. The sample was then imaged using a tapping mode SFM system (Digital Instruments, Santa Barbara, CA) in air (*6*).

In the tapping mode, the SFM tip oscillates up and down at a frequency of a few hundred kilohertz so that it makes transient contact with the sample at the bottom of its swing (*46*, *47*). The effect of the sample is then to clip the amplitude of the oscillation. As the sample is scanned underneath the tip, it can be raised or lowered to maintain the magnitude of this clipping constant. In this way, a topographic image of the sample can be obtained, while the lateral forces, which can push aside weakly adsorbed molecules, are largely eliminated (*48*, *49*). This mode of operation makes it possible to visualize samples under ambient humidity (*50*) or in a liquid environment (*51*, *52*).

Three parameters were used to chraracterize the effect of poly(ADP-ribosyl)ation on chromatin fibers observed with the SFM: the nucleosomal center-to-center distance (ccdist), the fiber width, and the fiber volume. The center-to-center distance and the width were measured using an image analysis program written in Matlab (MathWorks, Natick, MA), developed by M. Young and C. Rivetti (University of Oregon). To measure the volume of a chromatin fiber in a SFM image, the background of the image was first smoothed, and its height was set to zero. Then, the volume of a fiber was calculated as the sum of the products of the area and the height value of all pixels encompassing the fiber. The volume values were normalized against the volume of single nucleosomes in the same image, to correct for the effects of different tip dimensions. A computer routine in C was developed for the determination of the volume of chromatin fibers in an SFM image. The errors in the volume measurements were relatively large for the following two reasons. First, the background smoothing and the tip size affect the single nucleosome and the larger fibers somewhat differently, limiting the effectiveness of the normalization process. Second, the individual nucleosomes cannot be identified unambiguously in some images. To overcome the variability observed for different fibers, with different samples and in different experiments, data acquired from various parts of the fiber, from many different fibers and samples, were used to realize a significant comparison of these parameters.

Statistical Analysis. Statistical analysis was performed on the measured values of the nucleosomal center-to-center

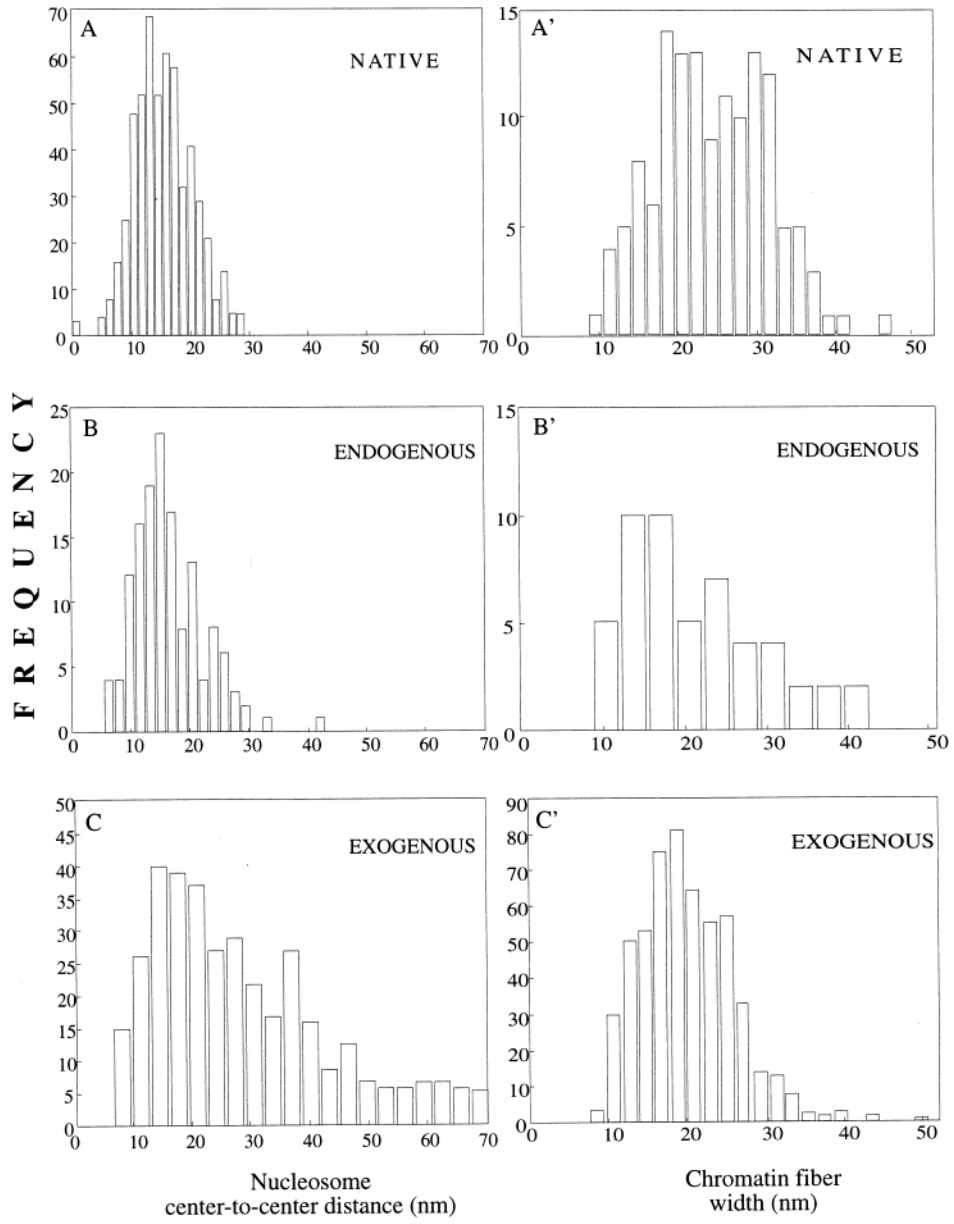

FIGURE 2: Frequency distribution histograms of the center-to-center internucleosomal distances (ccdist) and fiber widths. The histograms depict the distribution of center-to-center distances (ccdist) for (A) native fibers, (B) endogenously poly(ADP-ribosyl)ated chromatin fibers obtained by the addition of 200 μM NAD, and (C) exogenously poly(ADP-ribosyl)ated fibers obtained with two different concentrations of chromatin (see Experimental Procedures). Fiber widths of the same samples are shown in panels A′, B′, and C′, respectively. Each measure contains more than 200 points.

Table 1: Parameters of Chromatin Fibers from Chicken Erythrocyte Nuclei Analyzed by SFM Imaging[a]

	A	B	C	D	E	F	G	H
width (nm)[b]	25 ± 7	37 ± 7	21 ± 7	29 ± 7	20 ± 7	25 ± 7		
ccdist (nm)[b]	15 ± 4	<9	20 ± 7	<9	30 ± 15	26 ± 15	33 ± 12	25 ± 9
volume (nucleosomes/nm)	0.34 ± 0.05	0.51 ± 0.83	0.20 ± 0.12	0.23 ± 0.1	0.26 ± 0.02	0.18 ± 0.12	0.08 ± 0.02	0.10 ± 0.03

[a] Statistical analysis of chromatin fibers in the native state (A), in the native state with 10 mM $MgCl_2$ (B), poly(ADP-ribosyl)ated with endogenous PARP (C), poly(ADP-ribosyl)ated with endogenous PARP with 10 mM $MgCl_2$ (D), poly(ADP-ribosyl)ated with exogenous PARP (E), poly(ADP-ribosyl)ated with exogenous PARP with 10 mM $MgCl_2$ (F), in stripped chromatin fibers (G), and in stripped chromatin fibers with 10 mM $MgCl_2$ (H). [b] $p < 0.001$ (see the Results).

distance, of the fiber width, and of the fiber volume analysis using SPSS version 10 software (SPSS Inc., Chicago, IL). The results were expressed as the average values ± the standard deviation. Statistical comparison between measured values from fibers prepared differently was performed using a Student's *t* test, where the difference in the average values was considered significant when p was <0.05.

RESULTS

Effect of Poly(ADP-ribosyl)ation on Chromatin Structure. SFM images of native chromatin fibers revealed three-dimensional structures (Figure 1a). These images are similar to those reported previously by Leuba et al. (*5*), who also showed that there were no significant morphological differ-

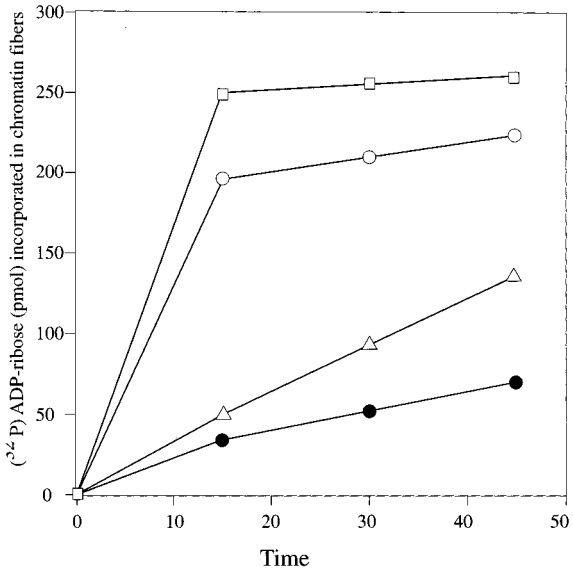

FIGURE 3: ADP-ribose incorporation at different concentrations of $MgCl_2$. Chromatin fibers (500 μg/mL) were incubated for 15 min at 30 °C in the presence of 5 units of poly(ADP-ribosyl)polymerase, 200 μM NAD, 2 μCi of [^{32}P]NAD (●), and different concentrations of $MgCl_2$: (△) 2, (○) 4, and (□) 10 mM.

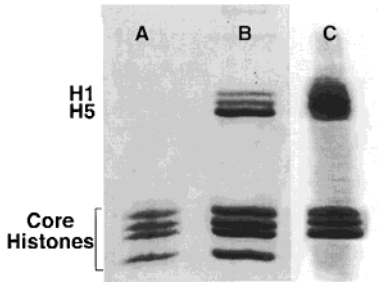

FIGURE 4: SDS−PAGE analysis of histones and H1-depleted chromatin fibers. (A) H1-depleted chromatin. (B) Native chromatin. (C) Autoradiography of ^{32}P-labeled poly(ADP-ribosyl)ated chromatin.

ences between the fibers in the fixed and unfixed samples. Significantly, the exogenous samples, in which the chromatin fibers were poly(ADP-ribosyl)ated in the presence of PARP (Figure 1c), revealed structures noticeably more uncoiled and relaxed than those observed in native chromatin fibers (Figure 1a) or in endogenously modified samples in which the modification is due only to the endogenous enzyme (Figure 1b).

The quantitative analysis of the data (Figure 2 and Table 1), indicates that the average center-to-center distance between nucleosomes increases from ~15 nm in the native fibers to 30 nm in exogenously poly(ADP-ribosyl)ated fibers. Similarly, the average fiber width decreases from 25 nm in the native fibers to 20 nm in the exogenously treated samples. In the endogenously modified samples (Figure 2 and Table 1), the average center-to-center distance between nucleosomes increases from 15 nm in the native fibers to 21 nm, while the average fiber width decreased from 25 to 21 nm.

Statistical analyses performed by the comparison between all the ccdist values of native chromatin fibers with the same measures of endogenous and exogeneous samples have given the following results: $p = 0.004$ and $p = 0.000$, respectively. Comparing the width of chromatin fibers for the same set of samples, we achieved a p of <0.001.

Despite a different variability of the deviation standard for the ccdist and width (Table 1), the statistical analyses have shown that these values were greatly significant.

To better characterize the changes in the structure of the inherently three-dimensional fiber structure, we measured the volume of the fibers and determined their nucleosomal linear density. This parameter decreases from a value of 0.34 nucleosome/nm for untreated chromatin (Table 1) to a value of 0.26 nucleosome/nm for poly(ADP-ribosyl)ated fibers. These data again indicate that poly(ADP-ribosyl)ation induces a transition in chromatin fibers from a more compact state to a more relaxed one.

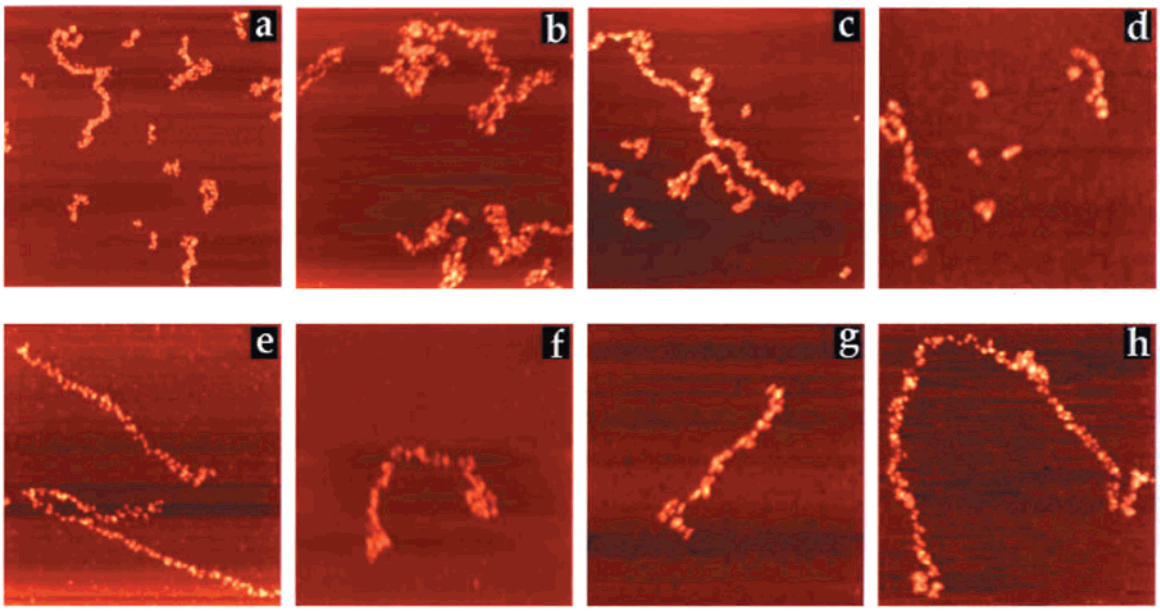

FIGURE 5: AFM images of chicken erythrocyte chromatin fibers at different concentrations of $MgCl_2$. (a−d) Chromatin fibers incubated with 0, 2, 4, and 10 mM $MgCl_2$, respectively. (e−h) Exogenously poly(ADP-ribosyl)ated chromatin fibers incubated with 0, 2, 4, and 10 mM $MgCl_2$, respectively. All the fibers were glutaraldehyde-fixed, deposited from 5 mM triethanolamine-HCl (pH 7.5) on mica, and imaged in air. Images were (a−d) 1.5 μm × 1.5 μm and (e−h) 1 μm × 1 μm in size.

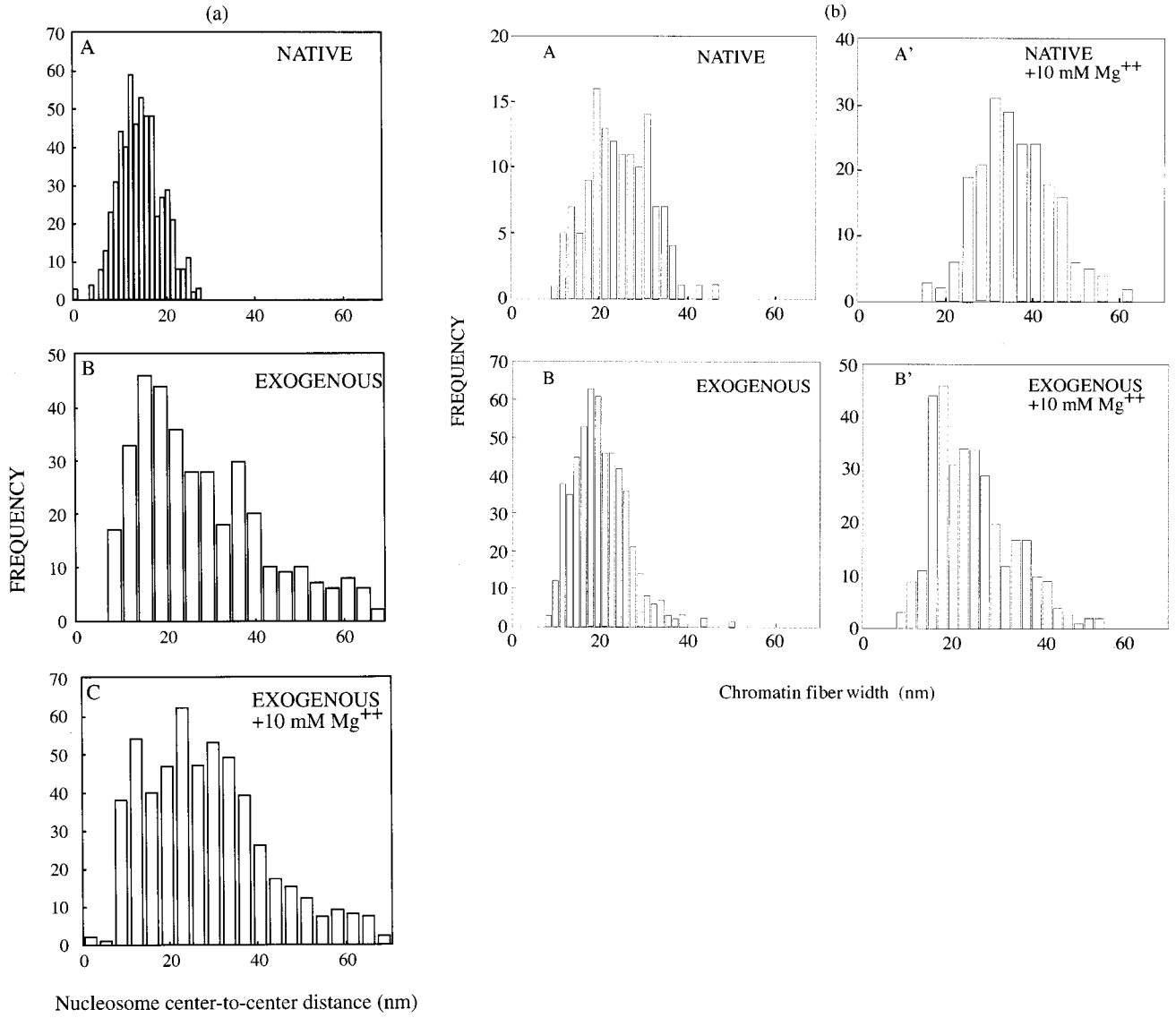

FIGURE 6: Frequency distribution histograms of the center-to-center internucleosomal distances (ccdist) and fiber widths. (a) Histograms displaying the distribution of center-to-center internucleosomal distances for (A) native chromatin fiber, (B) exogenously modified chromatin fibers (shown for comparison), and (C) exogenously modified chromatin fibers treated in the presence of 10 mM $MgCl_2$. (b) The histograms show the fiber widths of (A) native chromatin fibers, (A′) native chromatin fibers in the presence of 10 mM $MgCl_2$, (B) exogenously modified chromatin fibers, and (B′) exogenously modified chromatin fibers in the presence of 10 mM $MgCl_2$.

Effect of Mg^{2+} on Poly(ADP-ribosyl)ation and on Chromatin Structure. The enzyme poly(ADP-ribose)polymerase requires the presence of Mg^{2+} for optimal activity (*53*, *54*). Since Mg^{2+} itself is expected to increase the level of compaction of the fiber, it is of interest to establish the interplay between these two opposing factors on the fiber structure. To monitor the level of incorporation of poly(ADP-ribose) in the fibers, chromatin samples were poly(ADP-ribosyl)ated in the presence of PARP and [^{32}P]NAD, at various Mg^{2+} concentrations in the range of 2−10 mM (as indicated in Experimental Procedures). As expected, the enzyme activity was dependent on the concentration of Mg^{2+} (Figure 3). Autoradiography shows that the poly(ADP-ribose) moiety is mainly incorporated into H1/H5 histones and core histones (Figure 4).

Correspondingly, AFM images of native chromatin fibers showed a degree of condensation at increased Mg^{2+} concentrations (Figure 5b−d) higher than that observed in the absence of Mg^{2+} (Figure 5a). On the other hand, poly(ADP-ribosyl)ated fibers at the same Mg^{2+} concentrations (Figure 5f−h) appeared significantly less condensed than native fibers in the presence of Mg^{2+} but more condensed than chromatin fibers poly(ADP-ribosyl)ated in the absence of Mg^{2+} (Figure 5e). The quantitative analysis for the measured parameters is shown in panels a and b of Figure 6 and Table 1. This analysis reveals that the average center-to-center distance between nucleosomes of fibers that were poly(ADP-ribosyl)ated in the presence of 10 mM Mg^{2+} was 26 nm. In comparison, the distance between nucleosomes in fibers poly-(ADP-ribosyl)ated in the absence Mg^{2+} was ∼30 nm. The differences in the ccdist measures are statistically significant; in fact, a p of <0.001 was obtained. Concomitantly, the average width of chromatin fibers increased from 20 nm for chromatin fibers poly(ADP-ribosyl)ated in the absence Mg^{2+} to 25 nm for fibers poly(ADP-ribosyl)ated in the presence of 10 mM Mg^{2+}.

Stripped Chromatin Fibers and Mg^{2+}. To determine whether Mg^{2+} could also affect the structure of H1/H5-

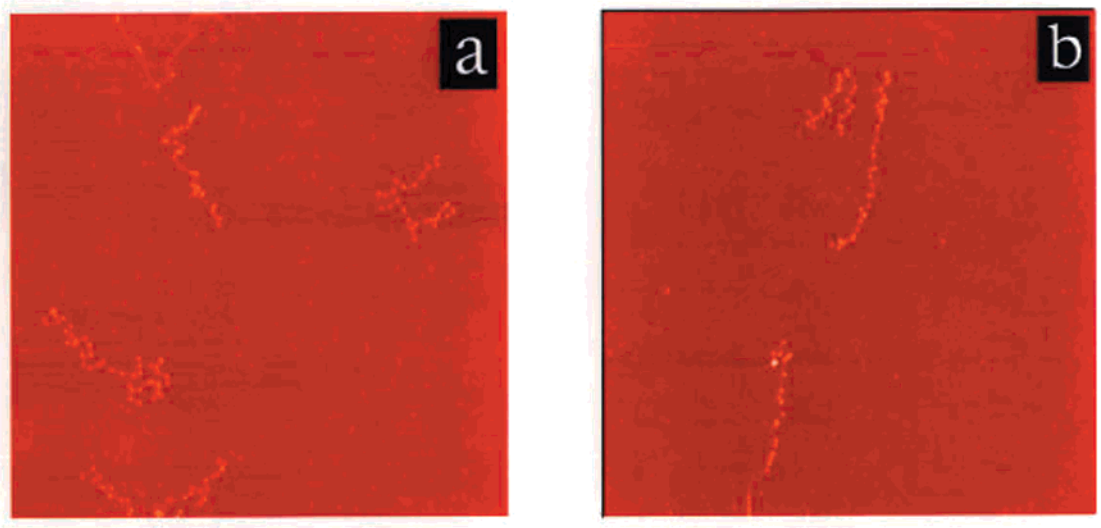

FIGURE 7: AFM image of H1/H5-depleted chromatin fibers: (a) stripped chromatin fibers and (b) stripped chromatin fibers in the presence of 10 mM $MgCl_2$. Images were 2 μm $\times$ 2 μm in size.

depleted chromatin, fibers were stripped of linker histones in the presence of 0.35 M NaCl, according to the method of ref *5*. Figure 4A shows that, following this treatment, the fibers display the gel electrophoresis pattern characteristic of stripped chromatin fibers. After exhaustive dialysis, the samples were imaged by AFM. As shown in Figure 7a, the images revealed the loss of the high-order structure in the stripped chromatin fibers which display the characteristic "beads-on-a-string" feature as previously observed (*45*). The addition of Mg^{2+} to the stripped fibers led to a partial condensation of the fiber (Figure 7b). An analysis of the images confirmed this finding; in particular, the average center-to-center distance between nucleosomes decreased from 33 nm in stripped chromatin fibers to 25 nm in stripped fibers treated with 10 mM Mg^{2+} (Figure 8**),** and these differences were statistically significant ($p < 0.001$).

DISCUSSION

Several studies on the molecular mechanism that regulates the folding and unfolding of chromatin during the cell cycle have shown that morphological changes in the high-order chromatin structure are driven through reversible modification of chromatin proteins (*55*, *56*). The process of poly(ADP-ribosyl)ation is thought to be involved in the dynamic transition of fibers between a condensed and a decondensed state through the addition of a negative charge to the nuclear proteins. To gain insight into the mechanism by which poly(ADP-ribosyl)ation alters the chromatin structures, we have used tapping-mode SFM to compare the structure of poly(ADP-ribosyl)ated fibers with the structures of their native counterparts.

The study presented here reveals that poly(ADP-ribosyl)ation of chromatin fibers induces fiber decondensation. These observations are consistent with the results obtained by De Murcia (*31*) on the effect of poly(ADP-ribosyl)ation on calf thymus chromatin fibers. However, our results do not support the possibility that poly(ADP-ribosyl)ation of H1 histone could act as a link among neighboring molecules leading to a compaction of chromatin (*57*). The larger internucleosomal distances observed in poly(ADP-ribosyl)ated fibers, when compared to those in native fibers, support the idea that poly(ADP-ribosyl)ation induces relaxation and decondensation of chromatin. This effect is correlated with the extent of ADP-ribosylation**,** as it has been observed, when endogenous poly(ADP-ribosyl)ated fibers were compared with the exogenous in vitro poly(ADP-ribosyl)ated ones.

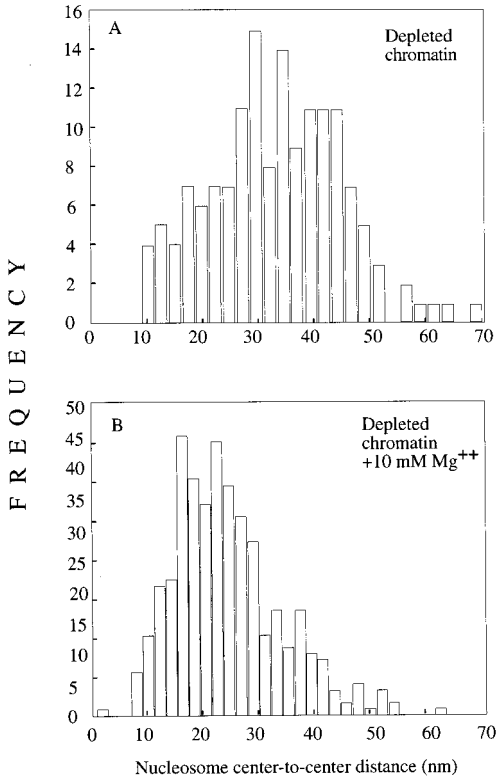

FIGURE 8: Frequency distribution histograms of center-to-center distances in H1/H5-depleted chromatin fibers: (A) stripped chromatin fibers and (B) stripped chromatin fibers in the presence of 10 mM $MgCl_2$.

It is likely that the extent of the relaxation depends on the amount of negative charges introduced by the poly(ADP-ribosyl)ation process (*9*, *58*). According to this hypothesis, the progressive addition of the ADP-ribose moiety could determine the extent of the partial dissociation of H1/H5 poly(ADP-ribosyl)ated histones from the fibers. This model

is consistent with the known effect of ionic strength on the state of compaction of the chromatin fibers (*59*−*61*).

The extent of chromatin compaction at a given ionic strength depends on the nature of the mono and divalent cations, and the presence of polyamines, etc., in the solution. The experimental data presented here for the effect of poly(ADP-ribosyl)ation as a function of Mg^{2+} clearly indicate a competition between the interaction of the opposite charges on the structure of the fibers. In fact, the internucleosomal center-to-center distance and the width of the fibers poly(ADP-ribosyl)ated in the presence of Mg^{2+} show that the modified fibers remain significantly decondensed, albeit to a lesser extent than poly(ADP-ribosyl)ated fibers in the absence of Mg^{2+}. The same conclusion could also be obtained from the comparison of the center-to-center distance of H1/H5 stripped fibers in the presence and absence of Mg^{2+}. Accordingly, the internucleosomal distance in the presence of the divalent ion is still significantly larger than that of the native fiber. Thus, Mg^{2+} alone cannot restore the native feature of the chromatin fiber without the presence of linker histones. All these results highlight the role of electrostatic interactions in modulating chromatin accessibility to the DNA repair enzymes or to the transcriptional machinery.

To gain more insight into the poly(ADP-ribosyl)ation mechanism, we have investigated whether the long negatively charged chains of ADP-ribose itself might facilitate the unfolding of chromatin fibers. The ADP-ribose polymers, at the concentrations used in the assays, were unable to induce any change in the chromatin conformation. This finding is in agreement with Thibault's results (*62*), suggesting that the covalent linkage between the protein and polymer is required to induce chromatin relaxation. However, these results do not support the suggestion of Mathis and Althaus (*63*) that free polymers can destabilize the core histones leading to the decondensation of the fiber.

The addition of poly(ADP-ribose) to the proteins could lead to a specific modification of their function by a combination of factors such as the size and branching structure of ADP-ribose polymers. Under our experimental conditions, autoradiography shows that both H1/H5 histones and the core histones are the main acceptors of poly(ADP-ribose). Experiments designed to reconstitute chromatin fibers by the addition of H1/H5 histones or of H1/H5 poly(ADP-ribosyl)ated isoforms indicate that H1/H5 proteins induce a condensation of chromatin fibers, while an opposite effect was observed with the poly(ADP-ribosyl)ated linker histones (data not shown). This observation suggests that poly(ADP-ribosyl)ation of linker histones is sufficient to induce chromatin decondensation. Further studies are needed to clarify the contribution of each poly(ADP-ribosyl)ated histone to the dynamics of high-order chromatin structure.

ACKNOWLEDGMENT

We are grateful to Prof. Roberto Strom for the helpful discussion. M.d. thanks all of Bustamante's laboratory and, in particular, Drs. Mark Young and Walker Chip for the help given in the SFM analysis. M.d. is also indebted to Dr. J. Zlatanova.

REFERENCES

1. Van Holde, K. E. (1988) *Chromatin*, Springer-Verlag, Heidelberg, Germany.
2. Bordas, J., Perez-Grau, L., Koch, M. H. J., Vega, M. C., and Nave, C. (1986) *Eur. Biophys. J. 13*, 158−173.
3. Woodcock, C. L., Grigoryev, S. A., Horowitz, R. A., and Whitaker (1993) *Proc. Natl. Acad. Sci. U.S.A. 90*, 9021−9025.
4. Woodcock, C. L., and Horowitz, R. A. (1995) *Trends Cell Biol. 5*, 272−277.
5. Leuba, S., Yang, G., Robert, C., Samori, B., Van Holde, K., Zlatanova, J., and Bustamante, C. (1994) *Proc. Natl. Acad. Sci. U.S.A. 91*, 11621−11625.
6. Yang, G., Leuba, S. H., Bustamante, C., Zlatanova, J., and van Holde, K. (1994) *Nat. Struct. Biol. 1*, 761−763.
7. Van Holde, K., and Zlatanova, J. (1995) *J. Biol. Chem. 270*, 8373−8376.
8. Bednar, J., Horowitz, R. A., Grogoryev, S., Carruthers, L., Hansen, J. C., Koster, A. J., and Woodcock, C. L. (1998) *Proc. Natl. Acad. Sci. U.S.A. 95*, 14173−14178.
9. D'Amours, D., Desnoyers, S., D'Silva, I., and Poirier, G. G. (1999) *Biochem. J. 342*, 249−268.
10. Boulikas, T. (1991) *Anticancer Res. 11*, 489−528.
11. Ueda, K., and Hayaishi, O. (1985) *Annu. Rev. Biochem. 54*, 73−100.
12. Durkacs, B. W., Omidiji, O., Gray, D. A., and Shall, S. (1980) *Nature 283*, 593−596.
13. Farzaneh, F., Zalin, F., Brill, D., and Shall, S. (1982) *Nature 300*, 362−366.
14. Boulikas, T. (1993) *Int. J. Oncol. 2*, 105−110.
15. Kaufmann, S. H., Desnoyers, S., Ottaviano, Y., Davidson, N. E., and Poirier, G. G. (1993) *Cancer Res. 53*, 3976−3985.
16. Simbulan-Rosenthal, C. M., Rosenthal, D. S., Ding, R., and Smulson, M. E. (1996) *Prog. Nucleic Acid Res. Mol. Biol. 55*, 135−156.
17. Simbulan-Rosenthal, C. M., Rosenthal, D. S., Iyer, S., Boulares, H., and Smulson, M. E. (1998) *J. Biol. Chem. 273*, 13703−13712.
18. de Murcia, G., and Menissier de Murcia, J. (1994) *Trends Biochem. Sci. 19*, 172−176.
19. Kreimeyer, A., Wielckens, K., Adamietz, P., and Hilz, H. (1984) *J. Biol. Chem. 259*, 890−896.
20. Althaus, F. R., and Richter, C. R. (1987) *Mol. Biol. Biochem. Biophys. 37*, 1−26.
21. Cleaver, J. E., and Morgan, W. F. (1991) *Mutat. Res. 257*, 1−18.
22. Quesada, P., D'Erme, M., Parise, G., Faraone-Mennella, M. R., Caiafa, P., and Farina, B. (1994) *Exp. Cell Res. 214*, 351−357.
23. Boulikas, T., Kong, C. F., Brooks, D., and Hsie, L. (1996) *Int. J. Oncol. 9*, 1287−1294.
24. Naegeli, H., and Althaus, F. (1991) *J. Biol. Chem. 266*, 10596−10601.
25. Panzater, P. L., Realini, C. R., and Althaus, F. R. (1992) *Biochemistry 31*, 1379−1385.
26. Realini, C. A., and Althaus, F. R. J. (1992) *J. Biol. Chem. 267*, 18858−18865.
27. Zardo, G., D'Erme, M., Reale, A., Strom, R., Perilli, M. G., and Caiafa P. (1997) *Biochemistry 36*, 7937−7943.
28. Wolffe, A. (1995) *Chromatin: structure & function*, 2nd ed., Academic Press, London.
29. Boulikas, T. (1988) *EMBO J. 7*, 757−767.
30. Thomas, J. O., and Kabaza, A. J. A. (1980) *Eur. J. Biochem. 112*, 501−511.
31. De Murcia, G., Huletsky, A., Lamarre, D., Gaudreau, A., Pouyet, J., Daune, M., and Poirier, G. G. (1986) *J. Biol. Chem. 261*, 7011−7017.
32. Huletsky, A., de Murcia, G., Muller, S., Hengartner, M., Menard, L., Lamarre, D., and Poirier, G. G. (1989) *J. Biol. Chem. 264*, 8878−8886.
33. Koch, M. H., Vega, M. C., Sayers, Z., and Michon, A. M. (1988) *Eur. Biophys. J. 16*, 307−319.
34. Hansen, J. C., Ausio, J., Stanik, V. H., and van Holde, K. E. (1989) *Biochemistry 28*, 9129−9136.

35. Hansen, J. C., and Wolffe, A. P. (1992) *Biochemistry 31*, 7977−7988.
36. Hammermann, M., Toth, K., Rodemer, C., Waldeck, W., May, R. P., and Langowsky, J. (2000) *Biophys. J. 79*, 584−594.
37. Libertini, L. J., and Small, E. W. (1980) *Nucleic Acids Res. 8*, 3517−3534.
38. Butsher, H. J., Auer, B., Klocker, H., Schweiger, M., and Hirsch-Kaufmann, M. (1986) *Anal. Biochem. 152*, 285−290.
39. Faraone-Mennella, M. R., Quesada, P., Farina, B., Leone, E., and Jones, R. (1984) *Biochem. J. 221*, 223−233.
40. Malanga, M., and Althaus, F. R. (1994) *J. Biol. Chem. 269*, 17691−17696.
41. Panzeter, P. L., and Althaus, F. R. (1990) *Nucleic Acids Res. 8*, 2194−2198.
42. Alvarez-Gonzales, R., and Jacobson, M. K. (1987) *Biochemistry 26*, 3218−3224.
43. D'Erme, M., Zardo, G., Reale, A., and Caiafa, P. (1996) *Biochem. J. 316*, 475−480.
44. De Lucia, F., Faraone-Mennella, M. R., D'Erme, M., Quesada, P., Caiafa, P., and Farina, B. (1994) *Biochem. Biophys. Res. Commun. 198*, 32−39.
45. Thoma, F., Koller, Th., and Klug, A. (1979) *J. Cell Biol. 83*, 403−427.
46. Bustamante, C., Erie, A., and Keller, D. (1994) *Curr. Opin. Struct. Biol. 4*, 750−760.
47. Bustamante, C., and Keller, D (1995*) Phys. Today 48*, 32−38.
48. Fritz, M., Radmocher, M., Cleveland, J. P., Allersme, M. W., Stewart, R. J., Gieselmanin, R., Janmey, P., Schmidt, C. F., and Hansma, P. K. (1995) *Langmuir 11*, 3529−3535.
49. Munoz-Butella, S., Martin, M. A., del Castello, B., and Vazquez, L. (1996) *Biophys. J. 71*, 86−90.
50. Hansma, H. G., Kim, K. J., Laney, D. E., Garcia, R. A., Argaman, M., Allen, M. J., and Parson, S. M. (1997) *J. Struct. Biol. 119*, 99−109.
51. Bustamante, C., and Rivetti, C. (1996) *Annu. Rev. Biophys. Biomol. Struct. 25*, 395−429.
52. Bustamante, C., Zuccheri, G., Leuba, S. H., Yang, G., and Samorì, B. (1997) *Methods 12*, 73−82.
53. Zahradka, P., and Ebisuzaki, K. (1984) *Eur. J. Biochem. 142*, 503−509.
54. Chen, Y. M., Shall, S., and O'Farrell, M. (1994) *Eur. J. Biochem. 224*, 135−142.
55. Cheung, P., Allis, C. D., and Sassone-Corsi, P. (2000) *Cell 103*, 263−271.
56. Wu, J., and Grunstein, M. (2000) *Trends Biochem. Sci. 25*, 619−623.
57. Jump, D. B., Butt, T. R., and Smulson, M. (1979) *Biochemistry 18*, 983−990.
58. Ferro, A., and Olivera, B. M. (1982) *J. Biol. Chem. 257*, 7808−7813.
59. Koch, M., Vega, M. C., Sayers, Z., and Michon, A. M. (1987) *Eur. J. Biophys. 13*, 157−163.
60. Carruthers, L. M., Bednar, J., Woodcock, C. L., and Hansen, J. C. (1998) *Biochemistry 37*, 14776−14787.
61. Howe, L., Iskandar, M., and Ausio, J. (1998) *J. Biol. Chem. 273*, 11625−11629.
62. Thibault, L., Hengartner, M., Lagueux, J., Poirier, G. G., and Muller, S. (1992) *Biochim. Biophys. Acta 1121*, 317−324.
63. Mathis, G., and Althaus, R. R. (1987) *Biochim. Biophys. Acta 143*, 1049−1054.

BI002742A